

# Cryocooler Reliability and Redundancy Considerations for Long-Life Space Missions

**R.G. Ross, Jr.**

Jet Propulsion Laboratory  
California Institute of Technology  
Pasadena, CA 91109

## ABSTRACT

One means of achieving high reliability with cryogenic payloads involving cryocoolers is to incorporate redundancy, either in the form of redundant coolers and/or redundant drive electronics. To access the redundant elements, electrical and/or heat switches must also be incorporated. Although the redundant elements protect against a possible failure, the increased system complexity and increased cryogenic load associated with the incorporation also have a negative effect on reliability that must be taken into account.

This paper presents an analysis of the reliability advantages and disadvantages of a variety of cryocooler redundancy options, based on their total reliability, mass, and power impact at the cryogenic system level. The paper begins with developing an approach for quantifying the probability of failure of the key subassemblies, such as coolers, electronics, and heat switches, associated with the redundancy; the analysis considers the subassembly's state of development, the complexity and testability of its critical failure mechanisms, and the effect of the total cryogenic load on its reliability. Means are also presented for estimating the total cryogenic load as influenced by the addition of the redundant elements.

Finally, the overall system performance (reliability, mass, and power) of the various cryocooler redundancy options is computed using the failure probabilities of the individual elements, and the system interrelationships of the elements.

## INTRODUCTION

Achieving high reliability is a key design driver for cryogenic systems required to provide continuous cooling during multi-year space missions. There are three key steps to achieving high reliability:

- 1) Use highly tested, robust components, such as cryocoolers and electronics that incorporate well understood design principles with a proven history of high reliability.
- 2) Thoroughly predict the cryogenic refrigeration load over the mission life-cycle and incorporate significant margin to cover load growth and cryocooler performance loss over time.
- 3) Incorporate redundant components to protect against individual component failures.

This said, the problem faced with most cryogenic systems is: "How do I assess the reliability of a one-of-a-kind cryocooler or cooler system component?" and "How do I trade off the reliabil-

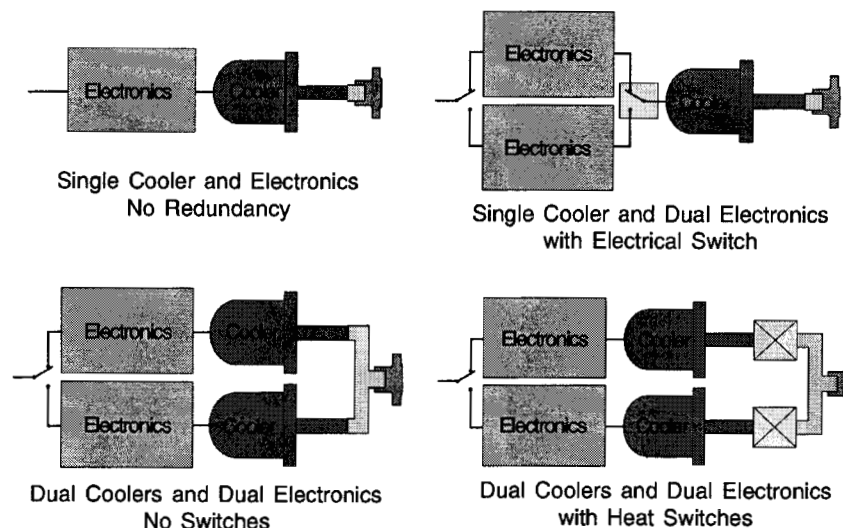


**Figure 1.** Example cryocooler redundancy options.

ity gain achieved from redundancy against the losses associated with increased system complexity and cryogenic load growth caused by adding the redundancy?"

The analysis presented in this paper was conducted to clarify these issues and provide a means for selecting an optimal configuration for a high-reliability cryocooler system. To help focus the discussion, Fig. 1 illustrates four example cooler system configurations.

In the sections that follow, the problem of assessing total cryogenic system reliability performance has been broken down into three computational steps: 1) quantifying the reliability (or probability of failure) of key cryogenic system subassemblies such as cryocoolers, cryocooler electronics, and heatswitches; 2) determining the total system cryogenic load associated with candidate redundancy options, and 3) quantifying the overall system performance associated with candidate cooler-system options including the mass and power performance of the overall system, and its overall reliability.

## ESTIMATING RELIABILITY OF KEY SYSTEM SUBASSEMBLIES

One of the most difficult issues is the problem of quantifying the reliability (or probability of failure) of an individual one-of-a-kind subassembly such as a cryocooler or heatswitch. Typically, such units are custom built for each application, and little or no quantitative reliability or life test data exist. For such subassemblies, one means of assessing their reliability is to first utilize expert knowledge of the unit's detailed design to identify each important failure mechanism associated with the unit's design features. This list will include such items as leakage of seals, fatigue of flexed elements, contamination of gasses, structural failure during launch vibration, etc.

Next, the probability of failure of each of these important mechanisms is estimated based on key attributes of the failure mechanism known to correlate with failure probability. These include:

- The extent to which the mechanism's underlying physics are well understood
- The level of complexity of the mechanism's parameter dependencies
- The accuracy of predictive analytical and experimental test methods that have been or will be used to design out the possibility of failure of the mechanism
- The degree to which the actual flight hardware can be and will be tested and validated with respect to the mechanism

The last step is then to combine the mechanism-level failure probabilities into a probability of failure for the total assembly level. For failure probabilities that are much less than one ( $P \ll 1.0$ ), the assembly-level probability of failure is well approximated as just the sum of the individual mechanism probabilities, i.e.  $P_{\text{assy}} = \sum P_i$  for all mechanisms  $i = 1, N$ . The reliability of a unit is just one minus the failure probability, i.e.  $R = 1 - P$ .

**Table 1. Benchmarks for Assessing Failure Probability.**

Failure Prob. (%)	Component / Mechanism Attribute
20	<b>High-level Concern.</b> High level of complexity of failure mechanisms, poor ability to thoroughly test, and a track record of failures. Example: first launch of a new launch vehicle.
10	<b>Significant Concern.</b> Modestly complex failure mechanisms often involving wearout or poorly understood physics, limited ability to thoroughly analyze and test, poorly quantified design margins, and previous failures of this type. Example: long-life space mechanisms involving continuous operation of complex components such as motors, gears, bearings, and slip rings.
5	<b>Modest Concern.</b> Known, but complex failure mechanisms including wearout and multiparameter dependencies, only modest ability to thoroughly test, some failures likely to occur. Often flown as redundant system to increase reliability. Example: S/C electronics
2	<b>Low-level Concern.</b> Known, but multifaceted failure mechanisms, relatively good ability to thoroughly test, but a track record of some failures slipping through. May be flown as redundant system to increase reliability. Example: thoroughly life-tested motor or mechanism.
1	<b>Important Issue, but not particularly a concern.</b> Well known failure mechanism, excellent ability to thoroughly test the actual flight hardware, and a solid track record of successfully resolving this issue. (Example: one-shot deployment mechanism with no extreme environments, and no poorly understood life-related or wearout issues)
0.5	<b>Modest Issue.</b> Failure mechanisms well understood, relatively mature predictive analysis and test techniques, and very few known failures of this type with qualified hardware. Generally accepted as single point failure. (Example: multilayer insulation for thermal control)
0.2	<b>Low-level Issue, failure very unlikely.</b> Very well known failure mechanisms, excellent predictive analysis and test techniques, well quantified but less conservative design margins, almost no known failures of this type with qualified hardware. Generally accepted as single point failure. (Example: highly optimized structures)
0.1	<b>Not really an issue, extremely unlikely.</b> Very well known mechanisms, excellent predictive analysis and test techniques, well quantified design margins, and almost no known failures of this type with qualified hardware. Almost always accepted as single point failure. (Example: S/C primary structure with conservative design margins)

To provide a consistent framework for making the mechanism-level failure probability assessments, Table 1 presents a series of benchmarks created by this author and drawn from experience with a broad variety of space hardware. Included in each failure probability level is a qualitative description of the attributes responsible for the assignment of that level.

### Cryocooler Reliability

As a first step in understanding cooler system reliability, it is useful to quantify the reliability of a variety of individual representative long-life space cryocooler types. The identified cryocooler failure mechanisms, shown in Table 2, are drawn from 10 years of personal knowledge of the development and testing of coolers at a number of space-cooler manufacturers, both in the U.S. and overseas. Similarly, the individual mechanism-level assessments are based on generic cooler sensitivities observed over the years. However, the mechanism-level failure probabilities reflect observations integrated over a number of similar cooler designs and must be corrected for any given design if that design has made a special effort to resolve a particular issue. As an example, Stirling coolers as a category suffer from a high sensitivity to side loading of the displacer coldfinger, which can cause internal rubbing and wear. However, some manufacturers, such as Raytheon, have greatly increased the robustness of their space-qualified Stirling-cooler displacers with respect to this issue and would deserve a much lower failure probability for "Expander blowby due to long term wear."

The qualitative data displayed in Table 2 not only provide a useful assessment of overall cooler reliability, but also provide insight into where to concentrate efforts to improve reliability. One can see that improved robustness with respect to contamination and leaks are key priorities drawn from this author's experience. Similarly, it can be seen that the use of pulse tube expanders has eliminated a number of failure mechanisms associated with Stirling expanders.

One aspect of cooler reliability not included in Table 2 is the sensitivity of cooler probability of failure to input power level. Sensitivity of reliability to power level is well known for driven mechanisms such as cars, planes, and motors, and one can project a similar sensitivity to power

**Table 2.** Failure Probability (%) of Mechanical Cooler Designs.

FAILURE MECHANISM	Pulse Tube w/ back-to-back Compressor	Pulse Tube w/ Compressor & Balancer	Stirling + Bal. w/ back-to-back Compressor	Dual Stirling w/ 2 Compres. & 2 Expand.
Excessive Internal Cooler Contamination	2	2	3	4
Hermetic Seal or Feedthrough Leak	2	2	2.5	3
Comp. Flexure Spring Breakage from Fatigue	0.1	0.1	0.1	0.1
Comp. Motor Wiring Isolation Breakdown	1	1	1	1
Comp. Piston Alignment Failure (Binding)	0.2	0.2	0.2	0.2
Comp. Piston Blowby due to Seal Wear	1	1	1	1
Compressor Piston Position Sensor Failure	1	0.7	1	1
Expander Structural Failure (e.g. at launch)	0.2	0.2	0.2	0.3
Expander Blowby due to Long-term Wear	0	0	3	4
Expander Motor Wiring Isolation Breakdown	0	0	0.5	0.5
Expander Spindle Alignment Failure (Binding)	0	0	0.2	0.2
Expander/Balancer Position Sensor Failure	0	0.7	1	1
<b>Total Failure Probability (%)</b>	<b>7.5</b>	<b>7.9</b>	<b>13.7</b>	<b>16.3</b>

level for some cooler failure mechanisms. It is important to assess this sensitivity because fraction loading level is an important trade-off parameter for cooler selection and sizing.

Table 3 presents this author's estimate of the effect of fraction piston stroke or fraction of maximum input power on the failure probability of the pulse tube cooler design introduced as the left-most column in Table 2. The various fraction power and fraction stroke column headings reflect the nonlinear drop in power which accompanies reduction in stroke. Note that the failure probabilities in Table 2 match the 85%-stroke operating point in Table 3; this is because an 85%-stroke is considered the nominal design point for a cooler. Also note that failure mechanisms such as leakage are unaffected by power level, whereas others such as contamination from piston rubbing are considered to be strongly dependent on input power and stroke.

### Cryocooler Electronics Reliability

In addition to the mechanical cooler itself, most cryocooler systems include a relatively complex set of cooler drive electronics used to generate the AC drive current from the 28 VDC spacecraft power bus, to control the cooler operation, and to communicate digitally with the host spacecraft or instrument. Although there are well developed ways of estimating electronics reliability, Table 4 presents an abbreviated assessment of probability of failure reflecting the four

**Table 3.** Failure Probability (%) vs. Power Level for Pulse Tube Coolers.

FAILURE MECHANISM	30% Power 65% Stroke	50% Power 75% Stroke	65% Power 85% Stroke	90% Power 95% Stroke
Excessive Internal Cooler Contamination	1	1.5	2	3
Leakage from Seal or Feedthrough Failure	2	2	2	2
Comp. Flexure Spring Breakage from Fatigue	0	0	0.1	0.2
Comp. Motor Wiring Isolation Breakdown	0.2	0.5	1	2
Loss of Piston Spindle Alignment	0.2	0.2	0.2	0.2
Comp. Piston Blowby due to Seal Wear	0.2	0.5	1	2
Compressor Piston Position Sensor Failure	1	1	1	1
Expander Structural Failure (during launch)	0.2	0.2	0.2	0.2
<b>Total Failure Probability (%)</b>	<b>4.8</b>	<b>5.9</b>	<b>7.5</b>	<b>10.6</b>

**Table 4.** Failure Probability of Cryocooler Electronics vs. Cooler Power Level.

FAILURE MECHANISM	30% Power 65% Stroke	50% Power 75% Stroke	65% Power 85% Stroke	90% Power 95% Stroke
Compressor Drive-Power Electronics Failure	1	1.5	2	3
Digital Control Electronics Failure	3	3	3	3
Analog Sensor Electronics Failure	1	1	1	1
Cooler Software Caused Failure	3	3	3	3
<b>Total Failure Probability (%)</b>	<b>8</b>	<b>8.5</b>	<b>9</b>	<b>10</b>

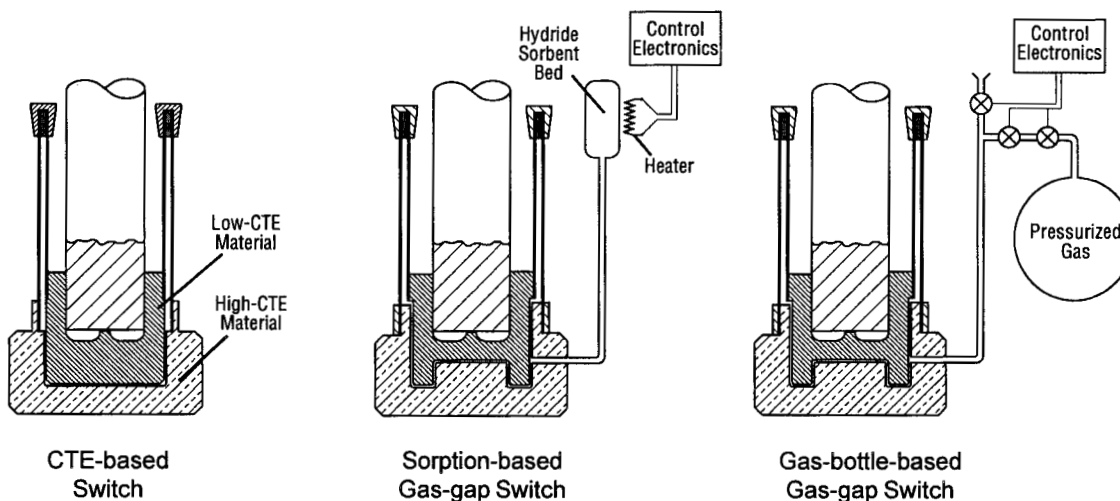
main ingredients of the cooler electronics including its power drive electronics, analog sensor electronics, digital control electronics, and controlling software. As with the mechanical cooler, power level has been included as a parameter to allow it to be used in subsequent trade studies.

### Heat Switch Reliability

The use of redundant cryocoolers generally involves the consideration of heat switches to isolate the thermal load of the turned-off (backup) cooler from the primary operating cooler, and to connect the backup cooler when it is needed. The off-cooler heat load is the heat conducted down the cold finger of the non-operating cooler, and it can be half of the total load if heat switches are not used. Because heat switches are generally considered to be relatively high-risk devices that add significant parasitic loads, heat switch reliability and performance must be fully included in any trade study of cooler redundancy options.

As shown in Fig. 2, there are three generic types of heatswitch designs that have received widespread attention: 1) the so called CTE-based switch, 2) the gas-gap thermal switch fed by a hydride sorption pump, and 3) the gas-gap thermal switch fed by bottled gas.

The CTE-based switch utilizes materials of widely different Coefficients of Thermal Expansion (CTE) to cause an outer element of a high-CTE material such as aluminum or copper to shrink tightly around a low-CTE material such as molybdenum or beryllium when the high-CTE material is cooled. The classic challenge with this design is the possibility of coldwelding of the mating surfaces over long time periods, and the fact that available CTEs result in the gap between the two materials being quite small ( $\sim 25 \mu\text{m}$ ). This small gap makes the design quite vulnerable to shorting out from small side loads. These reliability risk areas of the CTE-based thermal switch are highlighted in the right hand column of Table 5 and summed to achieve an estimated total failure probability for this design of about 7.5%.

**Figure 2.** Three generic heat switch options.

**Table 5.** Failure Probability of Various Heat Switch Designs.

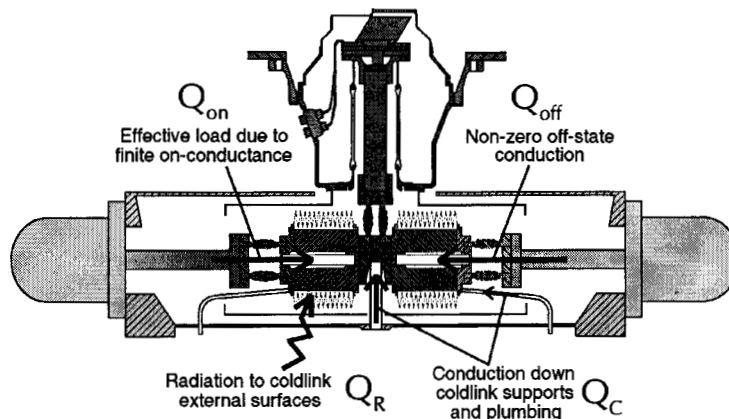
FAILURE MECHANISM	Bottle Fed Gas-Gas Switch w/ Redun.Valves	Sorption Based Gas-Gas Switch	CTE Driven Switch
<b>Switch Fails to Survive Launch</b>			
Critical gaps short due to system distortion during launch	0.5	0.5	0.5
Leak develops in gas actuation system	0.2	0.1	
<b>Switch Fails to OPEN after Long-Term Aging</b>			
Critical gaps short due to long-term warpage/creep	3	3	3
Gas evacuation system fails (valve failure or contaminant gases)	2	5	
Mating surfaces of CTE driven switch cold weld together			4
<b>Switch Fails to CLOSE after Long-Term Aging</b>			
Gas injection system fails (electronics, valves, or sorption heater)	1	1	
Loss of gas due to long-term leak	5	2	
<b>Total Failure Probability of Switch System (%)</b>	<b>11.7</b>	<b>11.6</b>	<b>7.5</b>

The second type of heat switch design, the gas-gap switch, is also based on maintaining a very small gap between the switch halves and therefore suffers from the same high sensitivity to side loading; however, in this case the gap is designed to be always open so that cold welding is not an issue. To actuate a gas-gap switch, a gas such as hydrogen is introduced into the gap to cause conduction across the gap. The required filling and evacuation of the gas has its own set of reliability issues, and these are noted in the gas-gap columns of Table 5.

In this author's assessment, the CTE-based switch is the more reliable of the three, but all have failure probabilities similar to the cryocooler they are designed to be integrated with. This low reliability prediction for heat switches is driven by the lack of good predictive analysis and test methods for failure mechanisms such as cold welding, long-term leakage, gaseous contamination, and small movements from warpage or side loads through flexbraids.

### ESTIMATING CRYOGENIC LOAD GROWTH DUE TO REDUNDANCY

In addition to the reliability of the individual cryocooler and heatswitch assemblies, another key consideration that must be included into a cryogenic system trade study is the increased cryogenic load associated with the introduction of redundant elements. As noted in Fig. 3, this load growth has four components: 1) thermal conduction down added structural supports and plumbing, 2) the radiation load to the external surfaces of added cold components, 3) the effective load due to the thermal drop across added 'on' heat switches and thermal flexbraids, and 4) the thermal conduction load through 'off' heatswitches and coolers.

**Figure 3.** Cryogenic loads associated with incorporating redundancy.

**Table 6.** Derivation of structural support conduction rule-of-thumb.

Instrument	Detector Mass (grams)	Detector Support Type	Standoff Temperature ( $\Delta T$ , K)	Conduction Load (mW)	Normalized Load $\mu\text{W/g}\cdot\text{K}$
TES	1000	Z-fold fiberglass tube	180-65=115	163	1.41
AIRS	597	hermetic glass tube	160-55=105	160	2.7
MICAS	570	taunt fiberglass band	140-100=40	48	2.1
Rule of Thumb	any	any	any	any	2.0

In a mature design, these loads could be computed with good accuracy based on the design details. However, for a generic trade study early in the design process, what is needed is a means of estimating each of these four loads based on rough sizing and mass estimates.

**Structural Support Conduction.** To estimate increased structural support conduction, what is desired is a generic relationship between overall support conductance and supported mass for typical launch loading conditions. This was derived by examining three flight-proven designs for cryogenic structural supports: one using a Z-fold fiberglass tube that supports the TES-instrument focal plane assembly, one using a hermetic glass tube that supports the AIRS-instrument focal plane assembly, and a third using taunt fiberglass bands that supports the MICAS-instrument focal plane assembly. Table 6 summarizes the very similar conductance computed for these three diverse designs and presents the derived rule-of-thumb conductance load of  $2 \mu\text{W}/\text{gram}\cdot\text{K}$ .

**Radiation Load.** Increased radiation load due to added cold surface area is estimated based on an effective emittance value of 0.05 for gold-plated surfaces or small-area MLI blankets typical of those used in a cryocooler cold-end assembly.

**Effective 'On-state Conduction' Load.** The effective 'On-state conduction' load is the additional load that a cooler would have to carry at a given cold-end temperature  $T_c$  to make up for the fact that it has to run colder (at temperature  $T_c - \Delta T$ ) because of the thermal drop  $\Delta T$  through a conducting heatswitch and/or thermal flexbraid assembly. This effective load ( $Q_{\text{on}}$ ) is sized to yield the same cooler input power with load ( $L + Q_{\text{on}}$ ) at temperature  $T_c$  as would be required with load ( $L$ ) at temperature ( $T_c - \Delta T$ ). This  $\Delta\text{load per } \Delta T$  is just the slope (watts/K) of the load curve for the cryocooler of interest. It can also be roughly approximated using Eq. 1, where the constant  $\mathfrak{R}$  varies from about 0.8 to 1.2 mW/W·K for typical high-efficiency space cryocoolers.

$$Q_{\text{on}} = \mathfrak{R} (\text{mW/W}\cdot\text{K}) \times \text{load (W)} \times \text{SP} \times \Delta T \quad (1)$$

In Eq. 1, SP is the specific power of the cryocooler at the cryogenic load temperature  $T_c$ , and  $\Delta T$  is the predicted temperature drop (K) through the 'On-state conductance'.

**Off-state Conduction Load.** The off-state conduction load down through a cryocooler cold-finger and 'off' heatswitch is computed from the combined 'off' thermal resistance of the cooler plus the heat switch. A typical value for a cryocooler 'off' thermal resistance is around 500 K/W, and a typical value for a heatswitch is in the range of 1000 to 2000 K/W.

## COMPUTING TOTAL SYSTEM-LEVEL THERMAL PERFORMANCE

At this point the necessary data have been generated to allow various cryocooler systems to be compared on the basis of total thermal performance. Once the thermal performance has been computed, the next section will then build up the total reliability performance.

To allow the various cryocooler redundancy options presented in Fig. 1 to be compared thermally, one needs to develop detailed conceptual designs for each system including realistic mass, size and parasitic-load estimates. This has been done for the four representative mechanical systems illustrated in Fig. 4. These systems include a single cooler with no redundancy, a redundant pair of coolers with CTE-based heat switches, and two variations of redundant coolers with no heat switches. In all cases, the cold end is assumed to be at 60 K and incorporates radiation shields tied to an assumed 160 K passively-cooled optical bench to minimize radiation loading of the 60 K cold-end surfaces. In the second case of redundant coolers with no heat switches, the

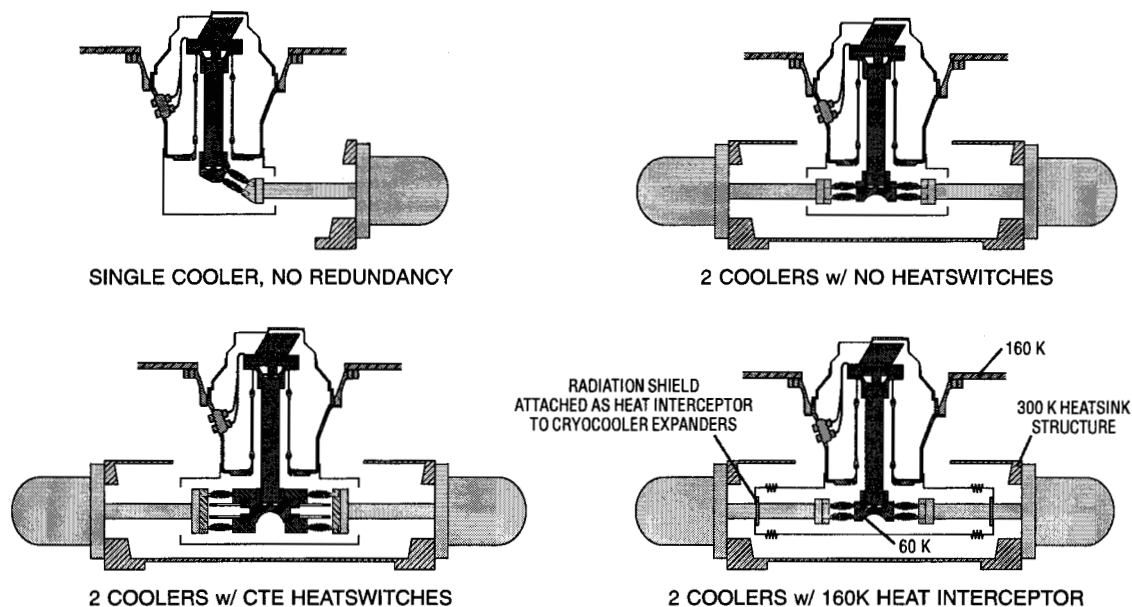


**Figure 4.** Conceptual designs of four cooler redundancy options.

160 K shield is also tied to both cryocooler coldfingers to act as a 160 K heat interceptor.<sup>1,2</sup> To allow its thermal performance to be assessed, each system has been drawn to scale and mated to a representative focal plane dewar assembly taken from the JPL AIRS instrument.<sup>3</sup>

For the case with the 160 K heat interceptor, the performance is assumed to follow the data measured at JPL for the MMS 80 K Stirling cooler as presented in Fig. 5.<sup>1</sup> From these data the use of a 160 K heat interceptor is seen to reduce the parasitic conduction load down through the non-operating cryocooler by 60%, and to also reduce the required input power of the operating cooler by around 40%.

Table 7 presents the computed thermal performance data for five cryocooler redundancy options: four with two redundant coolers (two with heat switches and two without), and one single cooler with no redundancy to serve as a reference.

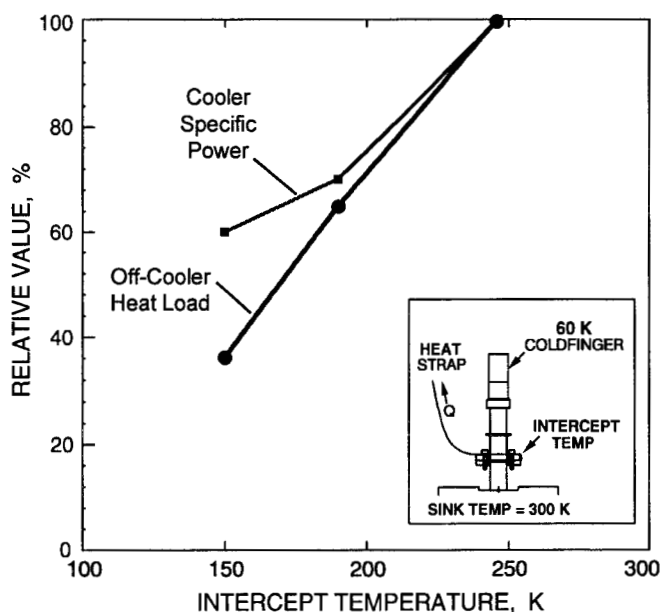


**Figure 5.** Measured performance gain at 60 K as a function of intercept temperature for the use of a heat interceptor on the MMS 80 K cryocooler.<sup>1</sup>

**Table 7.** Thermal Performance Comparison of Cooler Redundancy Options.

PARAMETER	2 Coolers CTE Switch 300 K sink	2 Coolers CTE Switch 160 K sink	2 Coolers No Switch 160K Ht Inter.	2 Coolers No Switch 160 K sink	1 Cooler No Redund. 160 K sink
Mass of a single heatswitch (g)	100	100	n/a	n/a	n/a
Total supported mass of coldlink assembly (g)	305	305	140	140	100
External surface area of single heatswitch (cm <sup>2</sup> )	80	80	n/a	n/a	n/a
Total cold surface area (A) for coldlink assembly (cm <sup>2</sup> )	120	120	100	100	65
Flexbraid/coupling "On" thermal resistance (K/W)	2.0	2.0	2.0	2.0	2.0
Heatswitch added "On" thermal resistance (K/W)	0.5	0.5	n/a	n/a	n/a
Total coldlink "On Thermal Resistance" ( $R_{on}$ ) (K/W)	2.5	2.5	2.0	2.0	2.0
Heatswitch "Off" Thermal Resistance ( $R_{off}$ ) (K/W)	1500	1500	n/a	n/a	n/a
Redundant Cooler "Off" Thermal Resistance ( $R_{off}$ ) (K/W)	500	500	500	500	n/a
Total coldlink support conduction from 160 K (mW)*	61	61	28	28	20
Total coldlink radiation load from sink (mW)**	275	22	19	19	12
Total "Off Cooler" heat load = $(T_H - 60) / (R_{off} + R_{off})$ (mW)	120	120	200	480	0
Total load from coldlink system (mW)	456	203	247	527	32
Baselined User Load at 60 K (mW)	500	500	500	500	500
Effective load due to total "On" Resistance (mW)***	91	49	45	129	22
Total Cooler Load ( $Q_c$ ) (mW)	1047	752	792	1156	554

\* Includes 1.2 K/W for second flexlink added to accommodate motion between 160 K sink and 300 K sink

\*Conduction Load (mW) =  $2 \times 10^{-3}$  (mW/g·K) × Cold Mass (g) ×  $\Delta T$ (K) (From Table 6)

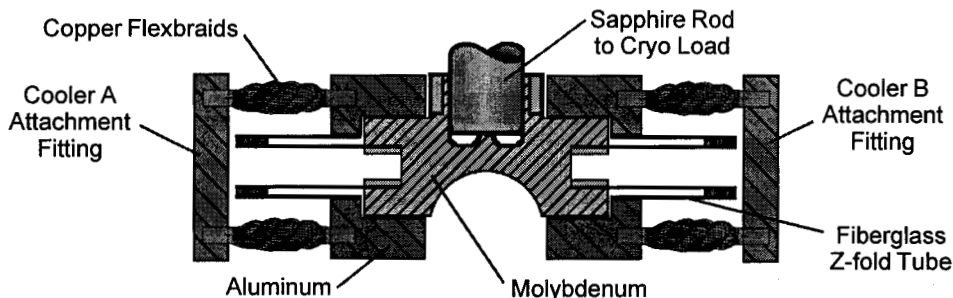
\*\* Radiation Load (mW):  $Q(\epsilon) \approx 5670 A \epsilon (T_{RAD,SINK}/1000)^4$ ,  $\epsilon \approx 0.05$

\*\*\* Effective "On Resistance" Load (mW) =  $1mW/W \cdot K \times [Total Load (W)]^2 \times R_{on} (K/W) \times Cooler Spec. Power (W/W)$  (From Eq. 1)  
Baselined Cooler Spec. Power @ 60 K= 40 W/W

The left-most two columns in Table 7 are for redundant cooler systems incorporating a JPL-designed dual CTE-based heatswitch shown in Fig. 6. The new conceptual design for a CTE-based heatswitch was specifically generated for this study because no heatswitch design was found in the literature that had useful performance. The concept shown in Fig. 6 was designed to yield a light-weight low-surface-area configuration with a Z-fold fiberglass tube that provides the needed rigidity to prevent a one-pound side load from shorting out the CTE gap. The side load itself is maintained below a pound by incorporating integral flexbraids into the cooler-attachment end of the switches; these flexbraids serve a double duty by also providing the needed flex coupling to the cooler coldfinger itself.

As shown in Fig. 4, the bodies of the switches are directly supported off of the 60 K focal-plane assembly as is done in the actual AIRS flight instrument; this minimizes conductive loads by making the structural conduction path to the 160 K optical bench instead of to the 300 K cryo-cooler support structure.

The difference between the left-most two columns in Table 7 is the existence or absence of a 160 K radiation shield surrounding the heatswitch assembly. In the left-most column, the 160 K radiation shield is absent, i.e. a background radiation temperature of 300 K is assumed for the heatswitch assembly surfaces. This 300 K background leads to a very high (~ 300 mW) parasitic radiation load, which is why all the other options have the 160 K radiation shield included.

**Figure 6.** JPL conceptual design for compact dual CTE-based heat switch.

Note that the total cooler load with these highly optimized heat switches and the 160 K shield is about 200 mW higher than the single non-redundant cooler, and about 400 mW less than the fully-redundant, no-heat-switch case. Thus, even these heat switches are only about 60% effective at removing the conductive load of the off-cooler. Other heat switch concepts in the literature<sup>4</sup> are much heavier and larger, and are therefore much worse.

The lesson learned is that heat switches must be low in external surface area, be light weight, and be enclosed with cryogenic radiation shields if they are to significantly reduce system parasitics associated with redundant coolers. Whereas a very good heat switch implementation may reduce parasitic loads by 50 to 70%, a poor heat switch implementation can lead to minimal load reduction, or may even increase parasitic loads.

In contrast to the use of heat switches, the center column of Table 7 describes the performance of dual coolers without heat switches, but with a heat interceptor at the radiation shield temperature. This concept is seen to offer parasitics comparable to the use of good heat switches, and also has the advantage of considerably improved cooler efficiency, as noted in Fig. 5.

## COMPUTING TOTAL SYSTEM-LEVEL RELIABILITY PERFORMANCE

Now that the assembly-level failure probabilities (Tables 2 - 5) and system-level thermal performance (Table 6) of the various redundancy options have been computed, this section combines these to compute the total system-level reliability performance. As a first step in this process it is useful to review the computational rules by which assembly-level failure probabilities combine to form system-level failure probabilities.

### System Reliability Computation

When various assemblies are connected in series and parallel to provide redundancy, the manner in which their reliabilities (or failure probabilities) combine is described by classic probability theory.<sup>5</sup> Although the definition of reliability is just one minus failure probability, the resulting equations used to combine reliabilities are more complex than the equivalent equations used to combine failure probabilities. For this reason, we have chosen here to use failure probability ( $P$ ), and not reliability ( $R = 1 - P$ ).

A typical cooler system, such as that shown in Fig. 7, is said to be made up of a series/parallel combination of elements or assemblies, each with a failure probability ( $P_i$ ). When  $P_i$  is small compared to one (say  $P < 10\%$ ), the combined failure probability of a series of assemblies (such as a cooler in series with a heat switch) is just the sum of their individual failure probabilities, i.e. ( $P_{\text{sys}} = \sum p_i$ ). This is true as long as the failures are statistically independent, i.e. the failure of one does not influence the failure of the others, and each must work for the system to work.

On the other hand, when multiple assemblies are placed in parallel so that the system works if any one parallel branch is functional, then the combined failure probability of the system is just the product of the individual failure probabilities, i.e. ( $P_{\text{sys}} = \prod p_i$ ).

Using these relationships, the combined failure probability of the system shown in Fig. 7 can be computed in terms to the cooler failure probability ( $P_C$ ) and heat switch failure probability ( $P_{\text{SW}}$ ) as  $P_{\text{sys}} = (P_C + P_{\text{SW}})^2$ . This computational methodology will be used to examine the system-level reliability of the various cryocooler redundancy options explored in Table 7.

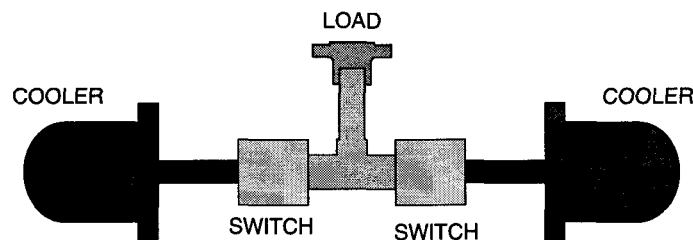


Figure 7. Classical dual cooler with heat switches configuration.

However, before doing that, it is instructive to examine a somewhat more complicated case to validate the accuracy of the derived relationship.

### CTE Heatswitch System Reliability

For the case where the heatswitches in Fig. 7 are CTE-based switches governed by the failure probabilities in Table 5, the data suggest that these switches tend to only fail shorted. Thus, a viable system can include a failed switch with an operating cooler together with a failed cooler with an operating switch. This two-failure case was explored using a more sophisticated statistical analysis techniques based on the binomial distribution function.<sup>5</sup> For this case it is found that one component failure is never a system failure, two thirds of two-failure scenarios are system failures, and all cases of three or four failures are a system failure.

For the case where the heat switch and cryocooler failure probability are equal, which is not an unreasonable assumption, the resulting system-level reliability is plotted in Fig. 8. From this figure it is seen that redundant coolers with no heat switches (e.g. AIRS), or 100%-reliable heat switches, provides significant reliability enhancement. Also, incorporation of heat switches with the same reliability as the cooler raises system failure probability 4X over systems with no switches.

### Reliability Summary for Cryocooler Redundancy Options

With the above background, we are now in a position to compute the overall system-level reliabilities and mass/power performance of the various cryocooler redundancy options presented originally in Fig 1. This is done in Table 8.

From this table it is seen that most of the redundancy options involving dual coolers or dual electronics roughly half the probability of failure of a single (no redundancy) cooler system. For the cases involving dual coolers, this is accompanied by a relatively large increase in system mass and power. The clear winner in this analysis is the option involving full redundancy, no heat switches, and the use of a 160 K heat interceptor to pick up the off-cooler parasitic loads and to improve the efficiency of the operating cooler.

## SUMMARY AND CONCLUSIONS

In this paper, an approach to cooler redundancy trade-offs has been developed and demonstrated. The approach includes mechanism-level assessment of the reliability of key system assemblies (coolers, switches, and electronics), includes reliability dependency on cooler power

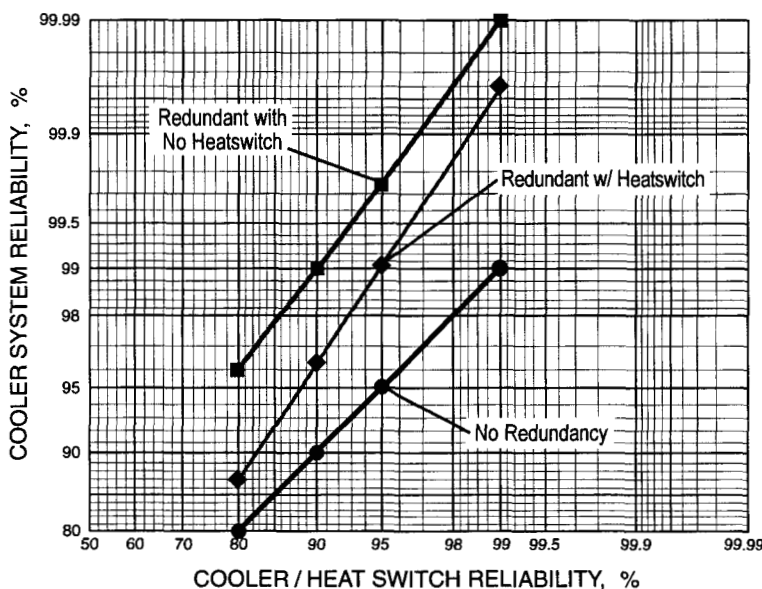


Figure 8. Affect of cooler redundancy on cooler system reliability.

**Table 8.** Overall Mass/Power/Reliability Comparison of Cooler Redundancy Options.

ITEM	2 Coolers w/ 2 Elect. (No Sw/h) w/ Heat Intercept.	2 Coolers w/ 2 Elect. w/ No Switches	2 Coolers w/ 2 Elect. w/ Heat Switches	1 Cooler w/ 2 Elect. w/ Elect. Switch	1 Cooler w/ 1 Elect. No Redundancy
COOLER POWER (watts)					
Total Effective Cryogenic Load (mW)	792	1156	752	554	554
Required Compressor Power* (W)	19.8	46.2	30.0	22.2	22.2
Compressor Power Level w.r.t. 50 W (%)	40	92	60	45	45
Cooler Electronics Power ( $\eta = 0.85 + 5W$ )	8.5	13.2	10.3	8.9	8.9
Total S/C Cooler-Related Bus Power (W)	28.3	59.4	40.3	31.1	31.1
COOLER MASS (per Instrument, kg)					
Mechanical Cooler(s)	8	8	8	4	4
Cooler Electronics, Switches & Cables	12	12	12	13	6
S/C System Mass Penalty (0.375 kg/W)	11	22	15	12	12
Total S/C Cooler-Related Mass	31	42	35	29	22
TOTAL SYSTEM FAILURE PROBABILITY					
Governing Equation	$P = (P_c + P_e)^2$	$P = (P_c + P_e)^2$	$P = (P_c + P_e + P_{sw})^2$	$P = P_e^2 + P_c + P_{sw}$	$P = P_e + P_c$
Cooler Failure Probability, $P_c$ (%)	5.0	10.6	7.5	5.0	5.0
Electronics Failure Probability, $P_e$ (%)	8	10	9	8	8
Switch Failure Probability, $P_{sw}$ (%)	n/a	n/a	7.5	1	n/a
Overall System Failure Probability (%)	1.7	4.2	5.8	6.6	13

\* Cooler specific power at 60K with 300 K sink = 40 W/W, with 160 K heat interceptor = 25 W/W

level, includes means of estimating increased parasitic loads associated with redundancy, and includes overall system mass, power, and cooling-load impacts.

Top level conclusions include: 1) The highest reliability is achieved with lightly-loaded, fully redundant coolers with heat interceptors to reduce the parasitic load, 2) the addition of heat switches can improve the system thermal efficiency somewhat, but with a significant increase in failure probability, 3) the use of redundant electronics only (with an electrical switch) has similar reliability to a system with heat switches, but with lower mass and power, and 4) a single cooler provides the lightest weight, lowest power, and least cost, but may have marginal reliability for a high-reliability mission.

## ACKNOWLEDGMENT

The work described in this paper was carried out by the Jet Propulsion Laboratory, California Institute of Technology, and was sponsored via Task Order 15144 by the National Oceanic & Atmospheric Administration (NOAA) National Environmental Satellite Data and Information Service (NESDIS) through an agreement with the National Aeronautics and Space Administration.

## REFERENCES

1. Johnson, D.L. and Ross, R.G., Jr., "Cryocooler Coldfinger Heat Interceptor", *Cryocoolers 8*, Plenum Press, New York, 1995, pp. 709-717.
2. Gilman, D.C., "Cryocooler Heat Interceptor Test for the SMTS Program", *Cryocoolers 9*, Plenum Press, New York, 1997, pp. 783-793.
3. Ross, R.G., Jr., et al., "AIRS PFM Pulse Tube Cooler System-level Performance," *Cryocoolers 10*, Kluwer Academic/Plenum Publishers, NY, 1999, pp. 119-128.
4. Bugby, D., et al., "Development of Advanced Cryogenic Integration Solutions," *Cryocoolers 10*, Kluwer Academic/Plenum Publishers, NY, 1999, p. 684.
5. ARINC Research Corp., *Reliability Engineering*, Prentice-Hall, Inc., Englewood Cliffs, NJ (1964).